Nanofriction of adsorbed monolayers on superconducting lead

M. Pierno, L. Bruschi, and G. Mistura*
Dipartimento di Fisica G.Galilei, Università di Padova, via Marzolo 8, IT-35131 Padova, Italy

C. Boragno, F. Buatier de Mongeot, U. Valbusa, and C. Martella
Dipartimento di Fisica, Università di Genova, via Dodecaneso 33, IT-16146 Genova, Italy
(Received 21 April 2011; published 28 July 2011)

With a quartz crystal microbalance (QCM) we have studied the nanofriction of neon and other simple gases deposited on lead at low temperature. Special care has been paid to the investigation of some artifacts in the QCM response encountered after the initial cooldown. Extensive results obtained with QCMs that have been thermally annealed confirm that Ne films slide on Pb below 10 K. However, no extra dissipation is observed when the Pb electrode is driven either magnetically or thermally into the metallic state. This means that the electronic contribution to friction is negligible for this system, probably, because of the small polarizability of Ne atoms. More polarizable adsorbates like N_2, Kr, and Xe are instead found to be completely pinned to Pb below 10 K.

DOI: 10.1103/PhysRevB.84.035448 PACS number(s): 68.35.Af, 68.47.De, 68.55.−a, 68.60.−p

I. INTRODUCTION

The common view of friction is that of a very important phenomenon from a practical point of view but scientifically dull. It is briefly mentioned at the beginning of any introductory physics classes where it is described in terms of simple empirical laws, which are said to be the results of many effects caused by the complexity of the two real surfaces in contact. The implicit message is that the sliding friction of an ideal system comprised by a very tiny particle lying on top of a flat uncontaminated surface kept in vacuum conditions will be trivial. Yet, investigations about the origins of friction are still scarce and controversial. For instance, if one asks whether friction depends on the conducting properties of the surface, he will not get a unanimous answer. In principle, if the substrate is metallic, there are two different processes through which a part of the kinetic energy of an object moving on a metal can be transformed into heat: the excitation of lattice vibrations and the induction of electron currents at the interface.[1] Despite recent advances[2] in experimental probes, the relative importance of these two contributions is still far from being settled. Quantifying this ratio experimentally has proven difficult because both the phononic and electronic dissipation channels are generally active. Recently, a change in friction was reported when a conducting tip of an atomic force microscope was moved over a silicon sample patterned with *p*- and *n*-doped regions at different voltage biases.[3] The mechanism for this variation is not clear but estimates of the electronic friction are far too low to explain the result.

Arguably, the most direct way to determine the importance of electronic friction is to work across the superconducting phase transition. When the substrate becomes a superconductor, the electronic mechanism is frozen out while that phononic one is essentially unaffected. Krim and coworkers have studied with a quartz microbalance technique (QCM) the friction between a lead substrate and an adsorbate film of solid nitrogen a few layers thick and found a sharp drop in friction by a factor ∼2 when Pb becames superconducting.[4] This work triggered significant debate because the observed behavior did not show the expected temperature dependence around the critical temperature T_c.[5,6] Furthermore, the same system was studied in a different QCM experiment[7] with improved cryogenics but complete pinning of the N_2 film to the Pb surface was reported in the temperature range 4–14 K. Subsequent measurements with a more controlled setup confirmed that N_2 films were quite susceptible to pinning.[8] More recently, the same group reported a drop of a factor ∼2 in friction for N_2 and He films on superconducting Pb.[9] However, in this experiment (i) the film coverage was not measured but only estimated, (ii) the superconducting state of Pb during the thermal scans was not directly probed, and (iii) the measurements were only taken during thermal warm-up cycles after cooling down the sample cell to 4.2 K. In a completely different experiment, Kisiel *et al.*[10] have studied noncontact friction on a niobium film across its T_c using a highly sensitive cantilever oscillating in the pendulum geometry in ultrahigh vacuum (UHV). They observed a reduction in the friction coefficient by a factor of three when the surface became superconducting and its temperature dependence was found to be in good agreement with theory.

In order to provide further data on this topic, we have studied with a quartz crystal microbalance technique the nanofriction of neon monolayers deposited on a bare lead surface across its T_c in a specially designed UHV system.[11] Unlike heavier adsorbates, Ne was found to reproducibly slide at such low temperatures.[12] However, no indication of a drop in friction was observed when Pb entered the superconducting state.[13] In our previous work, the QCMs had two Pb electrodes. Hereafter, we present more extensive results of this systematic study including those taken with new QCMs provided with one Pb electrode. Special care was paid to the investigation of some artifacts in the QCM response encountered at low temperatures. This paper is organized as follows. First, we describe in some detail the setup used for these measurements briefly specifying the technical improvements it presents with respect to other experiments. We then present the friction data acquired on various Pb surfaces, before summarizing the main results in the conclusions.

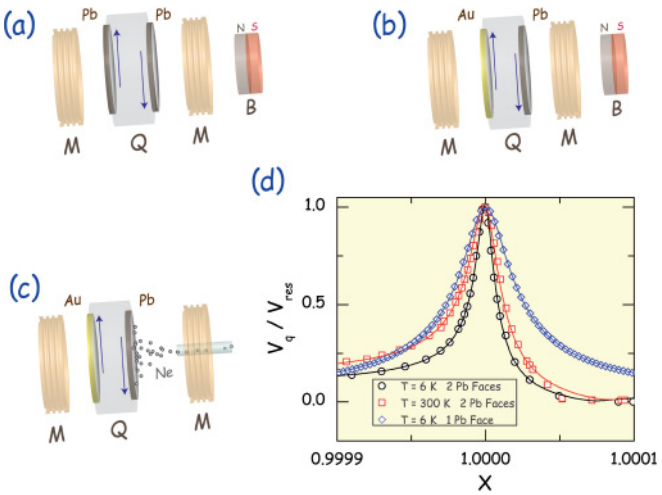

FIG. 1. (Color online) Sketch of the quartz crystal Q placed between two Meissner coils M and provided (a) with two Pb electrodes or (b) with one Pb and one Au electrodes. B indicates the permanent magnet. (c) Dosing of gas onto the Pb electrode. (d) QCM resonance curves in vacuum taken at two different temperatures and with different quartz crystals. Continuous lines are least-squares fits to the data.

II. THE EXPERIMENTAL SETUP

The microbalance is a small quartz disk whose principal faces are optically polished and covered by two metallic films [see Fig. 1(a)], which are used both as electrodes and as adsorption surfaces. Here, we mainly focus on crystals having one Pb electrode and one Au electrode [see Fig. 1(b)]. This design eliminates any possible spurious effects occurring when a nonuniform magnetic field B is applied on two Pb electrodes located at different distances from the magnet. The Pb electrodes have been grown by using a magnetron source in UHV conditions (base pressure 10^{-8} mbar).[12] Prior to Pb evaporation, the quartz crystals were polished and annealed. In order to obtain a final morphology characterized by large terraces, a high Pb flux (of the order of 5–10 nm/sec) has been used. The film thickness is in the range 200–300 nm. The morphology has been checked by *in situ* STM or *ex situ* AFM measurements, confirming the presence of (111)-terminated terraces, having a size peaked around 20 nm (larger terraces are also present in a significant percentage). Since during the QCM experiments the Pb electrodes were sometimes bombarded by ions to remove contaminants, an AFM topography has been also carried out on a sample used in several measurements. In this case, no relevant differences in morphology have been observed with respect to the as-deposited samples.

The quartz crystal is sandwiched between the two plates of a specially designed mounting.[11] With a wobble stick, the quartz crystal can be inserted in a copper receptacle attached to the cold finger of the main UHV chamber. The insertion/extraction of the QCM can be performed regardless of the temperature of the receptacle. This proves to be quite handy during the first cooldown from room temperature to avoid condensation of contaminants on the Pb electrodes. In the copper receptacle, the sample is placed between two Meissner coils M (see Fig. 1): one is driven by the reference output of a lock-in amplifier at ∼100 KHz and the other acts as a pickup coil. When the quartz electrodes become superconducting, the magnetic flux entrapped between the two coils is expelled and the induced signal drops. Close to the QCM, there is also a cog wheel provided with a strong permanent magnet [see Figs. 1(a) and 1(b)]. By turning the wheel with the wobble stick it is then possible to apply an external B to the Pb electrodes that may destroy the superconducting phase. A film is condensed onto the QCM and kept at low temperature by slowly leaking gas through a nozzle facing the QCM [see Fig. 1(c)]. It is then possible to study the system dissipation as Pb goes across the superconductor-metal transition induced either by the temperature variations or by the application of B.

The QCM presents a sharp mechanical resonance with the two parallel faces of the quartz plate oscillating in a transverse shear motion. The graph in Fig. 1(d) shows the normalized resonance curves of a quartz plate measured in vacuum at room temperature and at $T = 6$ K. To better compare the two curves, the horizontal axis, the frequency of the generator f, has been normalized to the resonance frequency $f_{\rm res} \sim 5$ MHz because $f_{\rm res}$ decreases by about 5 KHz upon cooling down the QCM from room temperature to $T = 6$ K. This quantity represents the series resonance of the RLC branch of the equivalent circuit of the QCM.[13] The vertical axis shows the corresponding amplified voltage V_q normalized to the peak value $V_{\rm res}$. The continuous lines are nonlinear least-squares fits to the data according to the formula

$$V_q^2 = V_0^2 \frac{[1 + Q_D(1-x)]^2 + \frac{Q_D^2}{4Q_s^2}}{1 + 4Q_s^2(1-x)^2}, \qquad (1)$$

where $x = f/f_{\rm res}$, V_0^2 is a constant that depends on the excitation voltage and the amplifier gain, Q_s is the series quality factor of the quartz, and $Q_D = f_{\rm res}/(f_p - f_{\rm res})$, where f_p is the parallel resonance at which the voltage across the quartz becomes minimum due to the presence of the capacitance between the electrodes C_0. In practice, V_0^2, Q_s, and Q_D are chosen as free parameters of the least-squares fits. For the resonance curves displayed in Fig. 1, Q_s is found to be 87 000 (55 000) at room temperature (low temperature) for the QCM with two Pb electrodes, while $Q_s = 38\,000$ for the case with one Pb electrode. The condensation of a film on the electrodes is signaled by a decrease of the resonance frequency $f_{\rm res}$. For instance, the shift estimated[12] for the deposition of a Ne monolayer on one face of the quartz crystals used in this study amounts to 2.3 Hz. Since the change in the quartz resonance after a cooldown from room temperature is reproducible within ∼200 Hz, it is necessary to measure the actual $f_{\rm res}$ of the bare QCM at the given T. Any dissipation taking place at the solid-film interface is detected by a decrease in the corresponding resonance amplitude.[14,15] The resonance frequency and amplitude are measured with the frequency modulation technique.[16]

III. EXPERIMENTAL RESULTS

More generally, we have found that for a reliable interpretation of the data, an accurate characterization of the behavior of the bare QCM is required. The graphs of Fig. 2 show representative temperature scans of the response in vacuum of a number of different quartz crystals having one or two

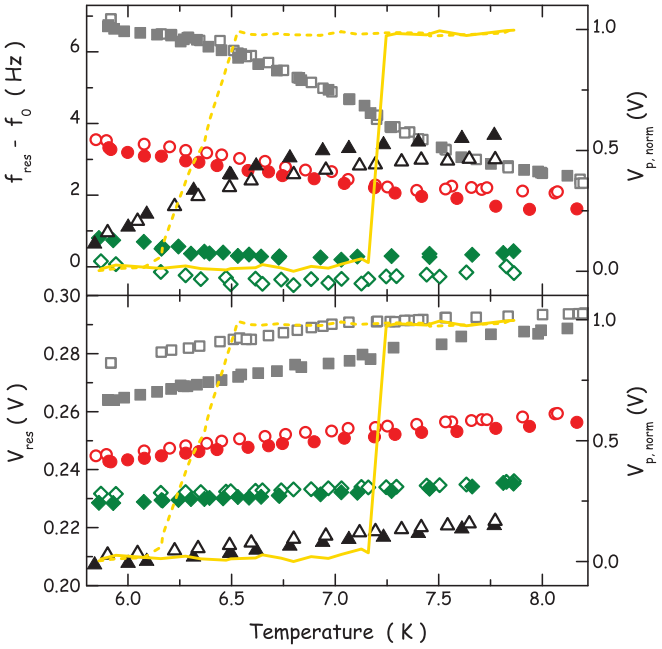

FIG. 2. (Color online) Temperature dependence of the resonance frequency (top graph) and amplitude (bottom graph). The resonance frequency is shifted with respect to the frequency of the bare crystal f_0. Full (open) symbols refer to points taken with (without) B. Different colors indicate different samples and/or different cooldowns. Lines represent the normalized pickup voltage in the presence (dashed line) and in the absence (solid line) of B.

lead electrodes measured right after the initial cooldown from room temperature. The top panel displays the dependence of the resonance frequency with (full symbols) and without (open symbols) the application of the external magnetic field. For clarity reasons, the initial frequency in zero field f_0 ($\sim$5 MHz) has been subtracted from each pair of scans and the two resulting curves have been vertically shifted by the same amount. These data show a complex, unpredictable behavior. For instance, $f_{\rm res}$ can increase (black symbols), decrease (gray and red symbols), or remain unchanged (green symbols) with increasing T. Similarly, the application of B can increase (green and black symbols), decrease (red symbols), or leave unchanged (gray symbols) $f_{\rm res}$. The continuous yellow line shows the dependence of the pickup voltage $V_{p,\rm norm}$ in arbitrary units corresponding to the green data points: the level 1 (0) indicates that the Pb electrode is in the normal (superconducting) phase. The $V_{p,\rm norm}$ data with no B indicate a sharp drop at a critical temperature $T_c = 7.2$ K, which is the expected value for Pb. The $V_{p,\rm norm}$ curves corresponding to the other samples have not been shown for clarity reasons. They all present sharp transitions with a T_c comprised between 6.9 and 7.2 K. The differences from the 7.2 K value are simply due to the temperature gradients existing between the QCM electrodes and the diode thermometer housed inside the copper receptacle.[13] As expected, the application of a B field lowers T_c and the transition becomes broader, see the gray dashed line. For all these QCMs, the thermal crossing of the superconducting transition is not signaled by any observable feature in $f_{\rm res}$.

The bottom graph shows the corresponding variations in the resonance amplitude. In contrast to $f_{\rm res}$, $V_{\rm res}$ is always found to increase monotonically with T and decrease with B, although the exact shift depends on the sample and/or cooldown. Interestingly, there is no sharp increase in $V_{\rm res}$ at T_c as we observed with a QCM provided with two Pb electrodes.[13] This is likely due to the larger series resistance that masks the change in electrical resistance of the Pb electrode at T_c. In fact, the Q_s of the crystals used to produce Fig. 2 are 3–5 times smaller than those reported before.[13]

Figure 3 shows the response of the bare QCM to a periodic application of B or to thermal jumps taken right after the initial cooldown. More precisely, panel A displays the variations in $f_{\rm res}$ (top graph) and in $V_{\rm res}$ (bottom graph) observed upon a periodic application of B at the constant temperature of 5.9 K. This causes an increase in $f_{\rm res}$ by about 0.5 Hz and a decrease in $V_{\rm res}$ by about 1% of the corresponding values measured with B off. The observed spikes are due to the turning of the wheel housing the permanent magnet. The red small stars indicate the stability of our temperature control while the continuous yellow line represents $V_{p,\rm norm}$. The fact that this signal is always low suggests that the Pb electrode is always in the superconducting phase and the application of B at $T = 5.9$ K is not sufficient to destroy this phase. Panel B shows instead the analog response of the same QCM taken at a slightly higher temperature of 6.6 K sufficient for the magnet to induce the transition to the metallic phase as indicated by the variations in $V_{p,\rm norm}$. Interestingly, the two panels A and B show the same behavior, suggesting that the observed jumps in $f_{\rm res}$ and $V_{\rm res}$ cannot be due to the crossing of the transition from superconducting to metallic Pb.

To further complicate matters, panel (C) in Fig. 3 displays the background of another crystal taken right after the initial cooldown where the frequency response to the application of B is the opposite than that seen in the previous panels: $f_{\rm res}$ now increases in the superconducting phase. A similar response in $f_{\rm res}$ was reported by Highland and Krim[9] in their QCM study of N_2, He, and H_2O films deposited on Pb electrodes. The sample cell was loaded with a certain amount of gas at relatively high temperatures (i.e., 85 K for N_2 and 300 K for H_2O), consequently cooled to 4.2 K and then allowed to warm across T_c while a periodic external B was supplied. The resonant frequency was found to be higher in the superconducting phase, which was taken as an indication of lower friction, and thus a more decoupled film.[9] Finally, panel (D) reports the response of the same crystal to the application of thermal jumps across T_c, which increase $V_{\rm res}$ and leave $f_{\rm res}$ unchanged, at variance with what we have reported before with annealed QCMs provided with two Pb electrodes.[13]

We believe that the mechanical stresses acting on the QCM after the initial cooldown are the main cause of the rich scenario we have just presented. This is confirmed by the fact that after a couple of thermal annealing cycles up to a temperature of about 50–60 K, the QCM response becomes highly reproducible. Figure 4 shows three consecutive isothermal scans indicating the slip time $\tau_{\rm slip}$ as a function of the coverage of Ne films deposited on bare Pb at 6.5 K. For the deposition, we used a Ne cylinder having a nominal purity of 5.0. These data were taken with the same quartz crystal whose resonance was shown in Fig. 1. In the absence of a vapor,[15] the slip time, which describes the viscous coupling between the substrate and the film, is derived from the shifts in the resonance frequency

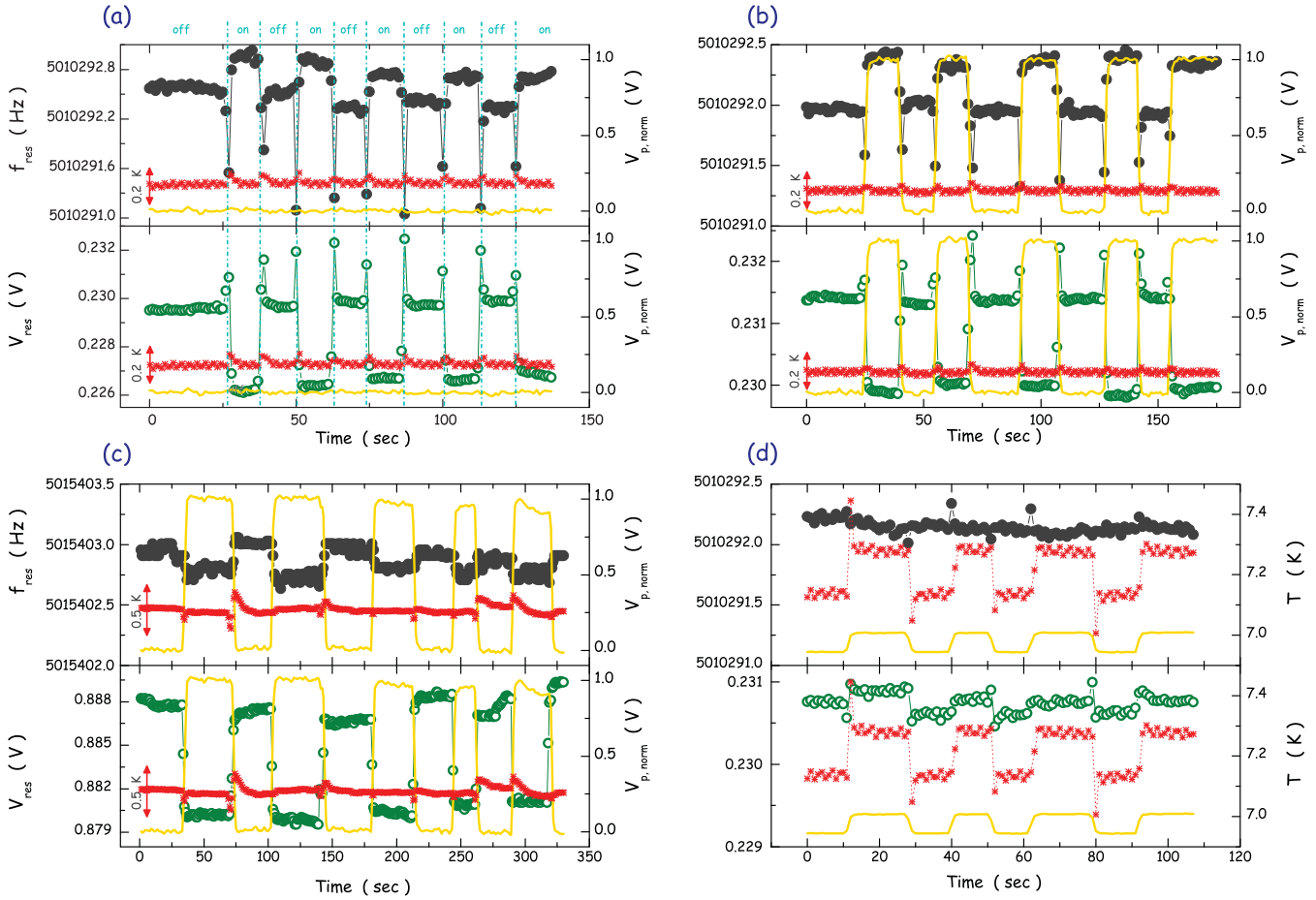

FIG. 3. (Color online) Response of bare QCMs to external perturbations. Time scale has been compressed by a factor 15. Top graphs in each panel show the QCM frequency (full dots, left axes) and the bottom graphs are the QCM amplitude (open dots, left axes). Continuous yellow lines represent the normalized pickup voltage (top and bottom graphs in each panel, right axes) and the red stars are the temperature (top and bottom graphs in each panel, vertical double arrows bars). Panel (a) shows the system response under the periodic application of B at $T = 5.9$ K, panel (b) under the periodic application of B at $T = 6.6$ K, same QCM, panel (c) under the periodic application of B at $T = 6.5$ K, different QCM, and panel (d) under the periodic variations in T (right axes), same QCM as in (a) and (b). For this panel, right axes show temperature, while the corresponding normalized pickup voltage (continuous line) oscillates between 0 and 1.

and amplitude of the QCM.[14] A very low τ_{slip} means high interfacial viscosity and, in the case of a film rigidly locked to the substrate, $\tau_{slip} = 0$. After each Ne deposition, the system was warmed up to ~60 K and cooled back down, the entire process lasting about 3 hours. The curves in Fig. 4 suggest an evolution in the QCM response; scan 1, taken right after the QCM was thermalized to 6.5 K after the initial cooldown from room temperature that requires about 12 hours, shows practically no slippage, scan 2 indicates a significant increase in τ_{slip} while scan 3 practically coincides with the previous one, suggesting that one thermal annealing may be sufficient to effectively remove the mechanical stresses caused by the initial cooldown to very low temperatures and get reproducible data. All the film's data discussed in this as well as previous works[13,17] refer to QCMs that underwent this annealing procedure. We add that a lot of quartz crystals were discarded because in the first Ne dosing runs, very little or no slippage was observed. Similarly, "working" QCMs showed no slippage after they were warmed up to room temperature for a couple of days and then cooled down again. We usually ascribed this behavior to unspecified contaminants, which covered the electrodes during the cooldown and/or during the measurements at low temperature and acted as very effective pinning centers. We now believe that most of these crystals would have detected slippage if they had been properly annealed.

With the new QCMs provided with a single Pb electrode we have monitored the dissipation during the deposition of Ne films and its dependence on variations in B and T, as we have done previously with QCMs having two Pb electrodes.[13] The results confirm that no extra dissipation is observed when the Pb electrode is driven either magnetically or thermally to the metallic state as we already reported.[13] To avoid showing very similar graphs, we present two scans that were not discussed in the previous work. Figure 5 shows the deposition of a Ne film onto a QCM having a single Pb electrode and the QCM response to the external B. Initially, the Pb electrode is bare at $T = 5.95$ K. At this temperature, $V_{p,\mathrm{norm}}$ is low, suggesting that Pb is in the superconducting phase. The application of B causes an increase in f_{res} and a decrease in V_{res} analog to Fig. 3(a), which cannot be due to the crossing of the superconducting transition, as indicated by $V_{p,\mathrm{norm}}$ that remains always at the zero level. At a time close to 20($\times$15) sec,

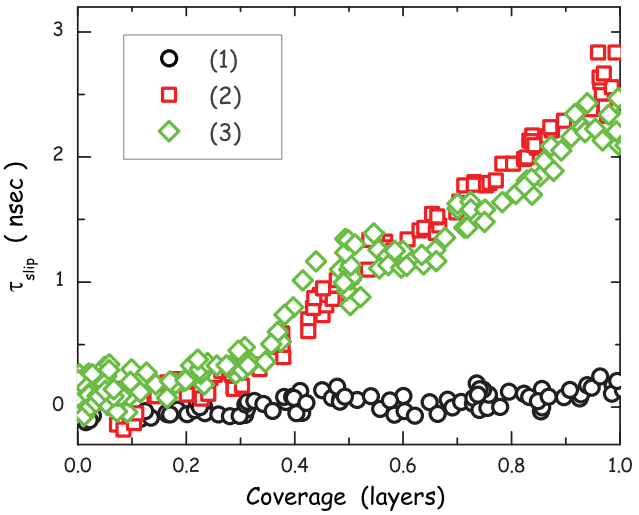

FIG. 4. (Color online) Slip time of Ne films deposited on bare Pb at $T = 6.5$ K. Data taken after (1) initial cooldown from room temperature, (2) one thermal annealing cycle to 60 K, and (3) two thermal annealing cycles to 60 K.

the sapphire leak valve is opened and this causes a linear drop in f_{res} due to the deposition of a Ne film, which is accompanied by a decrease in V_{res}. This increase in dissipation is attributed to the sliding friction of Ne over the Pb surface and it has been thoroughly characterized in previous publications.[12,17] After a frequency shift of about 3 Hz, corresponding[12] to a

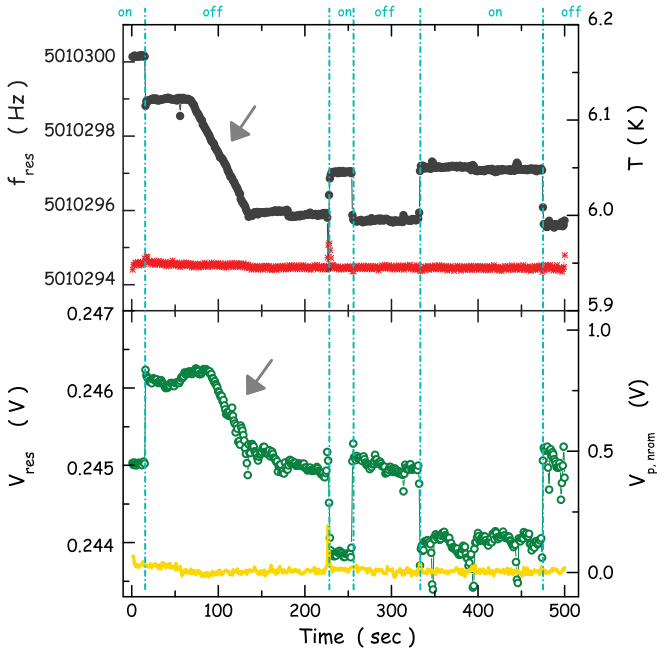

FIG. 5. (Color online) Time evolution of the quartz frequency (top graph, full dots, left axis) and amplitude (bottom graph, open dots, left axis). Time scale has been compressed by a factor 15. Red stars in the top graph represent the temperature, continuous yellow line in the bottom graph is the normalized pickup voltage. The corresponding scales are on the right axes. Vertical dashed lines are guides to the eye for visualizing the application (on) or removal (off) of B. Arrows indicate the dosing of Ne on Pb.

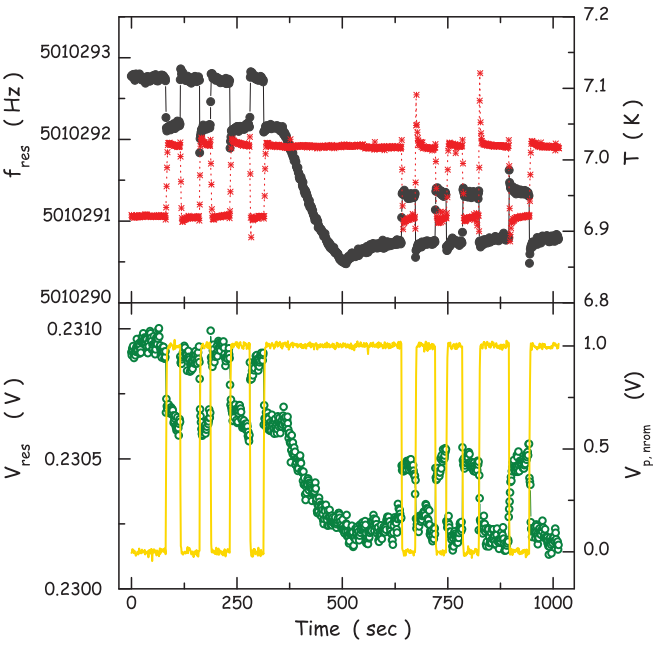

FIG. 6. (Color online) Time evolution of the quartz frequency (top graph, full dots, left axis) and amplitude (bottom graph, open dots, left axis) as a response of a cyclic temperature change (top graph, connected stars, right axis). Time scale has been compressed by a factor 15. Red stars in top graph represent the temperature, continuous yellow line in bottom graph the normalized pickup voltage. The corresponding scales are on the right axes.

film coverage of about 1.3 layers, the dosing valve is closed, the system is let to equilibrate and B is alternatively applied and removed. This causes a drop in the QCM amplitude and an increase in f_{res} whose values are quite similar to those observed without the Ne film.

Figure 6 shows the deposition of a Ne film on a different QCM having a single Pb electrode. Initially, the Pb electrode is bare and superconducting. Periodic temperature increases of ∼0.1 K drive the Pb to the metallic state. These shifts cause an increase in both f_{res} and V_{res}, a behavior different from those presented in Fig. 3. At a time close to 300(×15) sec, Ne is deposited on the QCM and V_{res} decreases as seen before. After a frequency shift of ∼1.5 Hz, gas dosing is stopped and the system is let to equilibrate. Afterwards, T is cycled across T_c and no extra dissipation is seen with respect to the bare QCM, in agreement with that found with all the other crystals. This shows that even though the response of a bare QCM may differ from sample to sample, it can be properly accounted for, so that consistent physical conclusions can be safely drawn.

IV. CONCLUSIONS

In summary, we have found that, after the initial cooldown from room temperature, the QCM responds in a variegated way to external stimuli. A thermal annealing cycle up to 50–60 K seems to effectively remove the mechanical stresses causing this behavior. The measurements with new QCMs that have only one Pb electrode have confirmed that the crossing of the Pb superconductor-metal transition is not accompanied by any extra dissipation due to electronic friction.[13] Obviously, our

study does not exclude the existence of such a contribution: it simply suggests that the electronic contribution to friction is negligible for this system probably because of the small polarizability of Ne atoms.[18] We have also tried to deposit more polarizable adsorbates like N_2, Kr, and Xe but we always found complete pinning below 10 K as reported before.[17,19] Molecular dynamics calculations[20] of a N_2 slab in contact with a Pb substrate indicate that below 25 K, the minimum force per molecule required to move the slab is several orders of magnitude larger than that typically achieved in QCM experiments, which is in agreement with the common observations of pinning of N_2 films on Pb at low T.[7,8,19] More recently, density-functional calculations[21] of Ne and Kr on Pb show that the activation energy of Ne is smaller than that of Kr, which leads to a large difference in their mobilities on Pb at $T < 7$ K. This may explain why Ne is found to systematically slide at such low temperatures, in contrast to the heavier rare gases. To overcome these limitations and thus to provide solid evidence of the electronic contribution to friction, it is then necessary to study superconducting QCM electrodes with a T_c significantly larger than that of Pb.

ACKNOWLEDGMENTS

We thank Giorgio Delfitto for his technical assistance. This work has been partially supported by MIUR-PRIN contracts Nos. 2006023721 and 2008Y2P573.

*giampaolo.mistura@unipd.it

[1] B. N. J. Persson, *Sliding Friction* (Springer-Verlag, Berlin, 1998).
[2] *Nanotribology: Friction and Wear on The Atomic Scale*, edited by E. Meyer and E. Gnecco (Springer, New York, 2007).
[3] J. Y. Park, D. F. Ogletree, P. A. Thiel, and M. Salmeron, Science **313**, 186 (2006).
[4] A. Dayo, W. Alnasrallah, and J. Krim, Phys. Rev. Lett. **80**, 1690 (1998).
[5] B. N. J. Persson and E. Tosatti, Surf. Sci. **411**, L855 (1998)
[6] B. N. J. Persson, Solid State Commun. **115**, 145 (2000).
[7] R. L. Renner, P. Taborek, and J. E. Rutledge, Phys. Rev. B **63**, 233405 (2001).
[8] B. L. Mason, S. M. Winder, and J. Krim, Tribol. Lett. **10**, 59 (2001).
[9] M. Highland and J. Krim, Phys. Rev. Lett. **96**, 226107 (2006).
[10] M. Kisiel, E. Gnecco, U. Gysin, L. Marot, S. Rast, and E. Meyer, Nat. Mater. **10**, 119 (2011).
[11] L. Bruschi, A. Carlin, F. Buatier de Mongeot, F. dalla Longa, L. Stringher, and G. Mistura, Rev. Sci. Instrum. **76**, 023904 (2005).
[12] L. Bruschi, G. Fois, A. Pontarollo, G. Mistura, B. Torre, F. B. de Mongeot, C. Boragno, R. Buzio, and U. Valbusa, Phys. Rev. Lett. **96**, 216101 (2006).
[13] M. Pierno, L. Bruschi, G. Fois, G. Mistura, C. Boragno, F. B. de Mongeot, and U. Valbusa, Phys. Rev. Lett. **105**, 016102 (2010).
[14] J. Krim and A. Widom, Phys. Rev. B **38**, 12184 (1988).
[15] L. Bruschi and G. Mistura, Phys. Rev. B **63**, 235411 (2001).
[16] L. Bruschi, G. Delfitto, and G. Mistura, Rev. Sci. Instrum. **70**, 153 (1999).
[17] L. Bruschi, M. Pierno, G. Fois, F. Ancilotto, G. Mistura, C. Boragno, F. Buatier de Mongeot, and U. Valbusa, Phys. Rev. B **81**, 115419 (2010).
[18] L. W. Bruch, Phys. Rev. B **61**, 16201 (2000).
[19] G. Fois, L. Bruschi, L. d'Apolito, G. Mistura, B. Torre, F. B. de Mongeot, C. Boragno, R. Buzio, and U. Valbusa, J. Phys. Condens. Matter **19**, 305013 (2007).
[20] M. Brigazzi, G. Santoro, A. Franchini, and V. Bortolani, J. Phys. Condens. Matter **19**, 305014 (2007).
[21] Y. N. Zhang, F. Hanke, V. Bortolani, M. Persson, and R. Q. Wu, Phys. Rev. Lett. **106**, 236103 (2011).